

# The Origin of the $\sigma$ -Hole in Halogen Atoms: a Valence Bond Perspective

Davide Franchini,<sup>[a]</sup> Alessandra Forni,<sup>\*,[b]</sup> Alessandro Genoni,<sup>[c]</sup> Stefano Pieraccini,<sup>\*,[a, b]</sup> Enrico Gandini,<sup>[a]</sup> and Maurizio Sironi<sup>\*,[a, b]</sup>

A detailed Valence Bond-Spin Coupled analysis of a series of halogenated molecules is here reported, allowing to get a rigorous ab initio demonstration of the qualitative models previously proposed to explain the origin of halogen bonding. The concepts of  $\sigma$ -hole and negative belt observed around the halogen atoms in the electrostatic potential maps are here interpreted by analysis of the relevant Spin Coupled orbitals.

The role of specific intermolecular interactions in driving self-assembling of molecular and macromolecular entities to build-up materials with selected properties and functionalities is largely recognized.<sup>[1]</sup> Rationalizing the nature of non covalent bonds and the mechanisms by which they act is therefore of paramount importance in view of designing new materials with improved performance and added value.

Among the interactions that have encountered wide success in materials science, halogen bond (XB)<sup>[2]</sup> has assumed a dominant position thanks to its recognized high directionality and selectivity, besides the attractive feature of being easily modulated. The latter property results from the possibility to vary not only the nature of the chemical environment bonded to the halogen (as it happens for hydrogen bond) but also the halogen itself. According to the IUPAC recommendation,<sup>[3]</sup> "A halogen bond occurs when there is evidence of a net attractive interaction between an electrophilic region associated with a

halogen atom in a molecular entity and a nucleophilic region in another, or the same, molecular entity." Halogen bond can be schematized as DX/A, where the moiety D bonded to the halogen atom X has a large variability, ranging from inorganic to organic species, and the nucleophilic site A is usually represented by a lone pair of a heteroatom such as oxygen, nitrogen, sulfur, or by a  $\pi$ -electron system such as, for example, that associated with a phenyl ring.

Though halogen bonding has been largely investigated from different points of view, at both theoretical and experimental levels,<sup>[2]</sup> a surprisingly low attention has been devoted to explain its physical origin. Indeed, at a first sight, this interaction can be considered as a quite unexpected and counterintuitive phenomenon: why should we have an attractive interaction between a typically electronegative atom and a nucleophilic site?

From a purely quantitative view the question can be answered by looking at the interaction energies as computed by both standard and more sophisticated ab initio methods: 'numbers' allow to get insights into the existence of the interaction and its strength. Even a very basic computational approach, such as a Hartree-Fock (HF) calculation (i.e. neglecting electron correlation) with a small basis set, is able to provide this information if no dispersive contributions are dominant. However, calculations do not respond to the need of qualitatively rationalizing the reason why this interaction is established. Chemists' understanding of reactions and recognition processes is always based on simple models that allow to predict the behavior of molecules. This is a crucial point for an efficient design of new molecules with desired properties and functions.


One of the first models to explain halogen bonding was proposed by Politzer and coworkers,<sup>[4]</sup> who highlighted an anisotropic distribution of the electrostatic potential (ESP) on the isodensity surface around a halogen atom X when covalently bonded to another atom Y. In particular, the ESP shows a positive region on X along the extension of the Y–X bond (the so-called  $\sigma$ -hole) and a negative belt perpendicular to the Y–X bond.


For a given DX molecule, the extent of such anisotropy depends on both the halogen type and the electron withdrawing capability of D. Specifically, the greater the polarizability of X the larger is the ESP anisotropy and, consequently, the strength of the interaction. It is therefore expected that the XB strength increases from chlorine to iodine, while fluorine is usually unable to give halogen bonding unless it is bonded to a strongly electronegative group. On the other hand, for a given

[a] Dr. D. Franchini, Prof. S. Pieraccini, Dr. E. Gandini, Prof. M. Sironi  
Department of Chemistry  
Università degli Studi di Milano and INSTM RU  
via Golgi 19  
20133 Milano (Italy)  
E-mail: stefano.pieraccini@unimi.it  
maurizio.sironi@unimi.it

[b] Dr. A. Forni, Prof. S. Pieraccini, Prof. M. Sironi  
SCITEC-CNR  
via Golgi 19  
20133 Milano (Italy)  
E-mail: alessandra.forni@scitec.cnr.it

[c] Dr. A. Genoni  
Université de Lorraine and CNRS, Laboratoire de Physique et Chimie  
Théoriques (LPCT), UMR CNRS 7019,  
1 Boulevard Arago  
Metz 57078 (France)

 Supporting information for this article is available on the WWW under <https://doi.org/10.1002/open.202000062>

 © 2020 The Authors. Published by Wiley-VCH Verlag GmbH & Co. KGaA. This is an open access article under the terms of the Creative Commons Attribution Non-Commercial NoDerivs License, which permits use and distribution in any medium, provided the original work is properly cited, the use is non-commercial and no modifications or adaptations are made.

halogen, the XB strength increases with increasing the electron withdrawing capability of D. The differences in the ESP anisotropies associated with different D groups can be discerned by comparing the maps of HCCBr and NCCBr (see Figure 1). In case of HCCBr, the presence of both the  $\sigma$ -hole along the extension of the C–Br bond, denoted by the narrow blue spot, and the belt of negative ESP around bromine, represented as a yellowish region, is evident. Going to NCCBr, only the former feature is observed. In fact, the stronger electron withdrawing CN group is responsible for a greater electronic transfer far from the Br atom, causing the disappearance of the negative belt around the halogen atom. Importantly, such features are reproduced even at the minimum level of theory.

A simpler (and more qualitative) model to explain halogen bonding, as well as the ESP anisotropy around the covalently bonded halogen atom, has been provided once again by Politzer and coworkers,<sup>[5]</sup> on the basis of the following argument related to the electronic structure of the halogen atom. The valence electronic configuration of X when bonded to Y along the z direction is  $s^2p_x^2p_y^2p_z^1$ . This configuration is responsible for a depletion of the electronic charge distribution in the z-direction (i.e., the bond axis) with respect to a mean value of 5/3 for the p electrons in each direction in the free halogen atom, so justifying the formation of the  $\sigma$  hole. The same configuration explains also a possible concentration of the electronic charge density in a belt around the Y–X bond.

Though these arguments based on the electronic configuration of the halogen atom to explain XB are commonly accepted in the chemists' community, they should be regarded as qualitative, suggesting the need of a rigorous first principles confirmation. To the best of our knowledge, this kind of investigation is still lacking in the literature.

The Valence Bond (VB) approach, where the nature of singly occupied orbitals can be rigorously determined in the frame-

work of ab initio methods, has often shown its advantages in examining and providing insights into fundamental chemical concepts.<sup>[6]</sup> It is therefore expected that the development of appropriate models to understand the nature of halogen bond can benefit from a VB investigation. To this aim, we report here a Valence Bond study of a series of halogenated molecules by using the Spin Coupled (SC) approach,<sup>[7]</sup> a VB technique where the orbitals are obtained without imposing any constraint in the full spin-space, i.e. considering all the possible chemical resonance structures (see SI for a brief overview of the SC theory). The SC method provides a fully correlated description of the electronic structure of a molecule, still preserving its interpretability in terms of the traditional chemical perception. Thanks to this appealing feature, this approach has been exploited to introduce, for the first time, correlated wavefunctions in the X-ray constrained wave function (XCW) approach,<sup>[8]</sup> giving rise to the new XC-SC strategy<sup>[9]</sup> which allows to extract chemically meaningful information from high-resolution X-ray diffraction data.

Starting from our recent SC investigation on a series of halogen bonded dimers, which confirmed previously proposed models and provided new insights into the nature of halogen bonding,<sup>[10]</sup> we focus here our attention on the electronic features of the XB donor. In particular we consider three DBr molecules, where D is either the hydrogen atom or the electron withdrawing groups HCC– or NC–, which are able to create the  $\sigma$ -hole on the halogen atom. Calculations have also been performed on the isolated bromine atom in order to discuss the changes in the orbital pictures going from the isolated atom to HBr and then to HCCBr and NCCBr. We will initially discuss the series Br, HBr, NCCBr since the HCCBr case introduces only smaller variations with respect to NCCBr.

The SC calculation on the free bromine atom gives rise to a pictorial description very close to the qualitative  $s^2p_x^2p_y^2p_z^1$  one. The corresponding squared SC orbitals are reported in Figure 2 (first column), where we obviously consider only one of the three equivalent solutions. The overlaps between all the pairs of orbitals are given in Table S1. The electron correlation between the motion of the electrons results into SC orbitals which describe the three lone pairs of the halogen atom using pairs of orbitals which are slightly different from each other. From Figure 2 it is evident that  $\varphi_1$ ,  $\varphi_2$  are essentially two s orbitals with different anisotropic expansion.  $\varphi_1$  is slightly more diffuse in the x and y directions, while  $\varphi_2$  is more expanded along z. The overlap between these orbitals is very high ( $\langle \varphi_1 | \varphi_2 \rangle = 0.96$ ).  $\varphi_3$  and  $\varphi_4$  are essentially  $p_x$  orbitals with a small additive ( $\varphi_3$ ) or subtractive ( $\varphi_4$ ) contribution of the s shell respectively, which describe the  $p_x^2$  lone pair.  $\varphi_5$  and  $\varphi_6$ , not shown in Figure 2, are the corresponding orbitals describing the  $p_y^2$  lone pair and can be viewed as obtained from  $\varphi_3$  and  $\varphi_4$  through a 90° rotation along the z direction. The overlap between the orbitals of the same lone pair is considerable ( $\langle \varphi_3 | \varphi_4 \rangle = \langle \varphi_5 | \varphi_6 \rangle = 0.80$ ) but lower compared to that of the  $\varphi_1$ ,  $\varphi_2$  pair, indicating a differentiation between  $p_x^2$  (or  $p_y^2$ ) and  $s^2$  pairs. On the other hand, the orbitals  $\varphi_3$  and  $\varphi_4$  have a small overlap with  $\varphi_5$  and  $\varphi_6$  ( $\langle \varphi_3 | \varphi_5 \rangle = \langle \varphi_3 | \varphi_6 \rangle = \langle \varphi_4 | \varphi_5 \rangle = \langle \varphi_4 | \varphi_6 \rangle = 0.02$ ) owing to their small s contribution. A

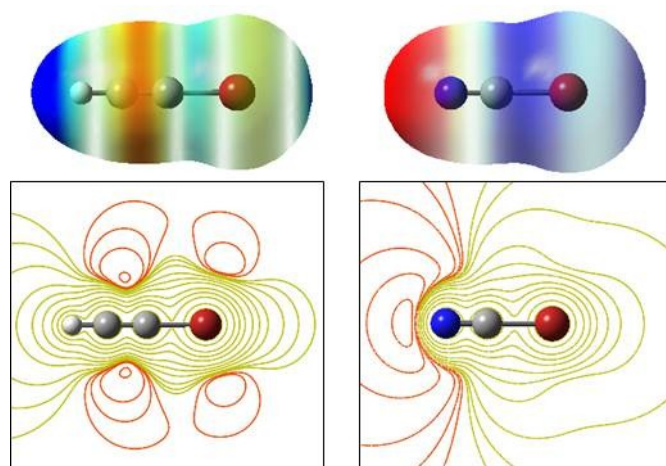


**Figure 1.** Electrostatic potential computed for HCCBr (left) and NCCBr (right) at HF/STO-3G level, the minimum level of theory. Top: maps on the 0.001 a.u. isosurfaces of electron density (values from  $-0.02$  au, red, to  $0.02$  au, blue). Bottom: contour levels drawn at  $\pm 2$ ,  $\pm 4$ ,  $\pm 8 \times 10^3$  au, with  $n$  as an integer ranging from  $-3$  to  $0$ ; positive values are denoted by yellow contours, and negative values are denoted by red contours.

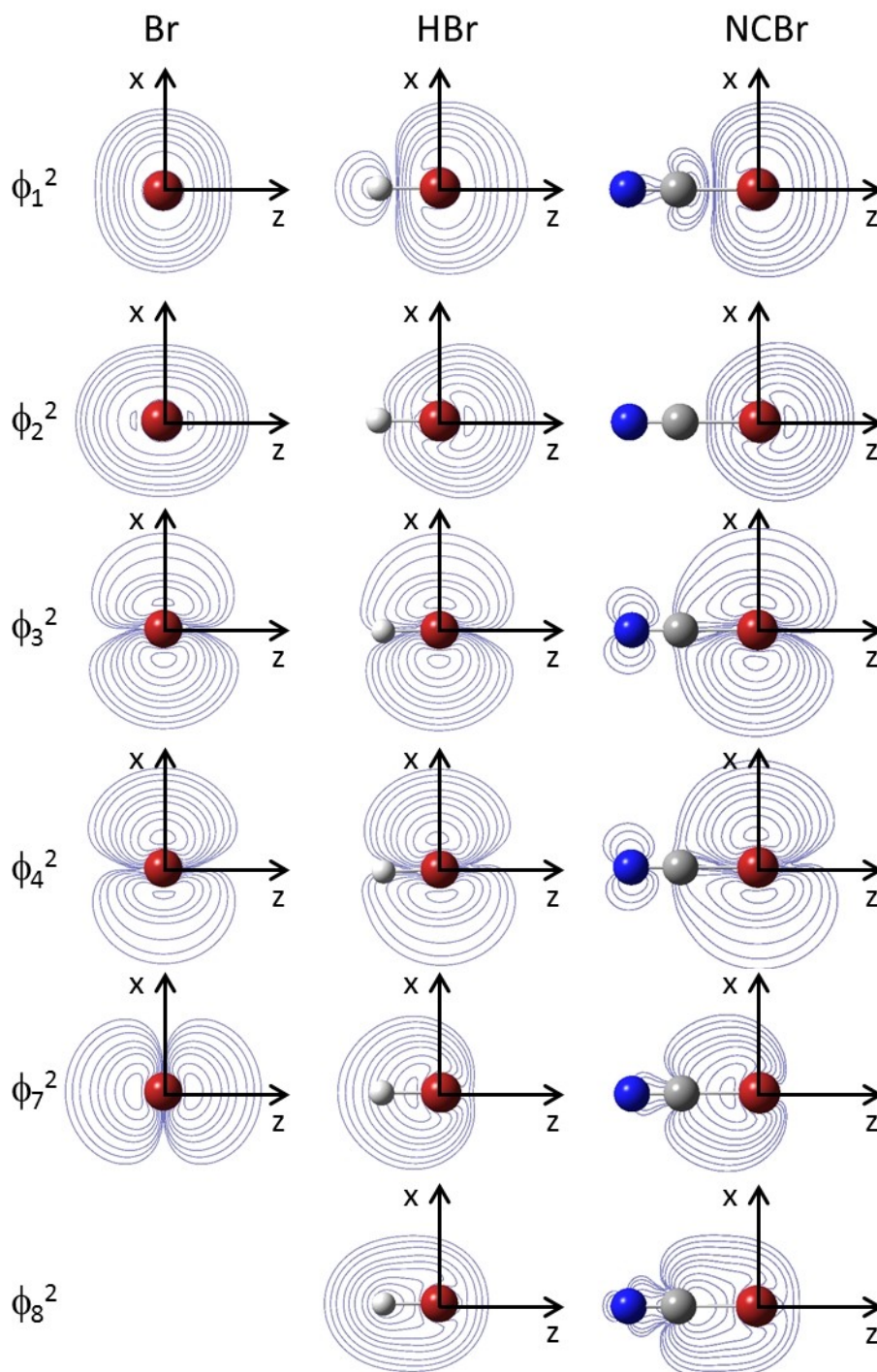


**Figure 2.** Plots of the squared symmetry-unique SC orbitals of Br, HBr and NCBr, with contour levels drawn at  $2, 4, 8 \times 10^9$  au, with  $n$  as an integer ranging from  $-4$  to  $0$ .

pure  $p_z$  orbital,  $\varphi_7$ , completes the set of the seven valence orbitals of the bromine atom. It should be noted that, though not clearly visible in Figure 2, the orbital  $\varphi_2$ , which is expanded along  $z$ , is slightly more diffuse than  $\varphi_1$ . Of course, this is due to the presence of only one electron in the  $z$  direction, differently from the  $x$  and  $y$  directions where four electrons are present. In

fact a SC calculation on the  $\text{Br}^-$  anion reveals the presence of two almost equivalent  $s$  orbitals with only a slightly different radial expansion.

Concerning the HBr molecule (see Figure 2, second column), with the hydrogen atom lying along the  $z$  direction, the three SC orbitals describing the  $s^2$  and  $p_z$  electrons, namely  $\varphi_1$ ,  $\varphi_2$  and



$\varphi_7$ , change their state becoming  $sp_z$  hybrid orbitals with different expansions:  $\varphi_1$  and  $\varphi_2$  tend to extend mainly outwards the H–Br bond preserving only a little tail in the region of the H–Br bond. Now the two orbitals describe what we could call an  $sp_z$  lone pair with high overlap between them (0.91). The  $\varphi_7$  orbital is mainly localized on the Br atom but heavily deformed toward the H atom. It has a large overlap (0.88) with the newly formed orbital,  $\varphi_8$ , which is also an  $sp_z$  hybrid orbital mainly localized on H and pointing toward Br. The  $\varphi_7$  orbital has also a significant overlap with the  $\varphi_1$  and  $\varphi_2$   $sp_z$  lone pair ( $\langle \varphi_7 | \varphi_1 \rangle = 0.60$  and  $\langle \varphi_7 | \varphi_2 \rangle = 0.46$ ).

The four  $\varphi_3$ – $\varphi_6$   $\pi$  orbitals are subject to a smaller rearrangement compared to the isolated Br atom. They are not pure  $\pi$  orbitals having a partial  $\sigma$  component, which is now due not only to the small  $s$  contribution (as in the case of the isolated Br atom) but also to a small  $p_z$  contribution. The nature of  $\varphi_3$  and  $\varphi_4$  can be shortly described as  $\varphi_3 = p_x + \lambda s + \mu p_z$  and  $\varphi_4 = p_x - \lambda s - \mu p_z$ , denoting with  $\lambda$  and  $\mu$  small weights coming from the  $\sigma$  components. Overall, the orbitals  $\varphi_3$  and  $\varphi_4$  describe the  $\pi_x$  lone pair, while  $\varphi_5$  and  $\varphi_6$ , which are symmetry-related to  $\varphi_3$  and  $\varphi_4$  through a  $90^\circ$  rotation around the  $z$ -axis, describe the  $\pi_y$  lone pair. The orbitals  $\varphi_3$  and  $\varphi_4$  are connected to each other by a reflection with respect to the  $yz$  plane. As these orbitals are essentially  $p_x$  orbitals, they have a high overlap between them ( $\langle \varphi_3 | \varphi_4 \rangle = 0.83$ ) and are practically orthogonal to the pair of  $p_y$  orbitals ( $\varphi_5$  and  $\varphi_6$ ). The very small overlap between the  $p_x$  and  $p_y$  pairs ( $\langle \varphi_3 | \varphi_5 \rangle = \langle \varphi_3 | \varphi_6 \rangle = \langle \varphi_4 | \varphi_5 \rangle = \langle \varphi_4 | \varphi_6 \rangle = 0.002$ ) arises from their small  $s$  and  $p_z$  contributions.

Looking at the spin pairing between SC orbitals, it results that the perfect pairing (i.e.,  $\varphi_1$ – $\varphi_2$ ,  $\varphi_3$ – $\varphi_4$ , ...,  $\varphi_7$ – $\varphi_8$ ) is the only predominant structure, followed by a much less important structure corresponding to the  $\varphi_1$ – $\varphi_4$ ,  $\varphi_2$ – $\varphi_4$ ,  $\varphi_5$ – $\varphi_6$ ,  $\varphi_7$ – $\varphi_8$  pairing.

Substitution of the H atom with the electron-withdrawing group CN (NCBr molecule, see Figure 2, third column) causes some small but important modifications in all the SC orbitals. To better appreciate these changes, we have also plotted (see Figure 3, first column) the differences of the squared orbitals,  $\varphi_{i,\text{NCBr}}^2 - \varphi_{i,\text{HBr}}^2$ . As expected, all orbitals undergo a contraction towards CN, because the high electronegativity of this group involves a depletion of electron density around the halogen, thus increasing the effect of its nuclear charge. In particular, the contraction of  $\varphi_1$  and  $\varphi_2$  manifests in the presence of positive  $\Delta\phi_1$ ,  $\Delta\phi_2$  regions along the  $z$ -axis in the region outwards the C–Br bond. Such orbital contraction can be therefore associated with the formation of the  $\sigma$ -hole in the electrostatic potential around the bromine atom (see Figure 1). The orbitals  $\varphi_1$  and  $\varphi_2$  still have a high overlap (0.90) and so they can be considered as a contracted  $p_z$  lone pair. As for the  $p_x$  lone pair, going from HBr to NCBr we observe only a small contraction in the  $x$  direction and an expansion in the region of the bond, resulting into almost negligible variations in the overlap of  $\varphi_3$  and  $\varphi_4$  with all the other orbitals and between each other. The same considerations are obviously valid for the  $p_y$  lone pair. The orbital  $\varphi_7$  extends much more in the  $z$  direction towards the C atom due to the electronegativity of the CN moiety and to the longer

C–Br bond distance compared to the H–Br one (1.786 vs. 1.400 Å, respectively), which requires a larger use of the more expanded  $s$  and  $p_z$  atomic orbitals in order to guarantee an efficient overlap with the  $\varphi_8$  orbital. The overlap  $\langle \varphi_7 | \varphi_8 \rangle$  remains indeed almost unchanged from HBr to NCBr (0.88 and 0.87 respectively).

The expansion of the orbital  $\varphi_7$  towards the C atom is also highlighted by a small reduction of its overlap with  $\varphi_1$  and  $\varphi_2$  ( $\langle \varphi_1 | \varphi_7 \rangle$  and  $\langle \varphi_2 | \varphi_7 \rangle$  decrease from 0.60 to 0.54 and from 0.46 to 0.38, respectively, going from HBr to NCBr). Finally, the substitution of the H atom with the CN group does not change the contribution of the spin structures, with the perfect spin pairing having always an overwhelming importance.

When comparing the squared orbitals of HCCBr and HBr, the plots of the  $\varphi_{i,\text{HCCBr}}^2 - \varphi_{i,\text{HBr}}^2$  differences appear to be almost indistinguishable from the  $\varphi_{i,\text{NCBr}}^2 - \varphi_{i,\text{HBr}}^2$  ones (see Figure S2).

On the other hand, if we compare the squared orbitals of NCBr and HCCBr, the same qualitative variations described above are observed, though to a lower extent. By looking at the differences of the squared orbitals,  $\varphi_{i,\text{NCBr}}^2 - \varphi_{i,\text{HCCBr}}^2$  (see Figure 3, second column), we can indeed observe a lower contraction of the orbitals, manifesting in: i) the formation of a positive region along the  $z$ -axis associated with the  $p_z$  lone pair (see  $\Delta\phi_1$ ,  $\Delta\phi_2$ ); ii) the predominance of the negative region around the bromine atom perpendicular to the bond axis, associated with the  $p_x$  lone pair (see  $\Delta\phi_3$ ,  $\Delta\phi_4$ ). Such negative region is overwhelmed by the positive one when bromine is bonded to stronger electron withdrawing groups (e.g. NC–), which further increase the contraction of all the orbitals.

These observations are in full agreement with what observed in the maps of the electrostatic potential (Figure 1). In fact, analysis of the ESP contour lines reveals a perfect matching between the positive region of ESP and the  $\Delta\phi_1$ ,  $\Delta\phi_2$  variations along the extension of the C–Br bond: the greater the  $\sigma$ -hole, the larger the positive  $\Delta\phi_1$ ,  $\Delta\phi_2$  regions. Moreover, the belt of negative electrostatic potential around the bromine atom, observed only for HCCBr, nicely corresponds to the low contraction of the  $p_x$  (and  $p_y$ ) lone pair, resulting into mainly negative  $\Delta\phi_3$ ,  $\Delta\phi_4$  (and  $\Delta\phi_5$ ,  $\Delta\phi_6$ ) region around the bromine atom. Such negative belt of ESP is lost in the NCBr case, for which the larger contraction of the  $p_x$  and  $p_y$  lone pairs implies a predominance of positive  $\Delta\phi_3$ , ...,  $\Delta\phi_6$  contributions.

It is worth mentioning that our analysis fully supports other interpretations of halogen bonding as found in the literature. As a first example, we cite the atomic interpretation provided by Scholfield *et al.*<sup>[11]</sup> in the development of force fields able to describe the anisotropy of the electrostatic potential around halogens. In their 'extended force field for biomolecular X-bonds', which involves the use of aspherical atomic charges and radii, the magnitude of the anisotropy has been interpreted by a displacement of the axis of the  $p_x$  and  $p_y$  orbitals with respect to the bond axis. Our SC study, providing a mixing of the  $p_x$  and  $p_y$  lone pairs with the  $\sigma$  components, leads to slightly bent orbitals with respect to the bond axis, in complete agreement with their conclusions. Another work reports the results of a DFT study on the interaction between halomethanes and rare gases,<sup>[12]</sup> leading to a different interpretation of the

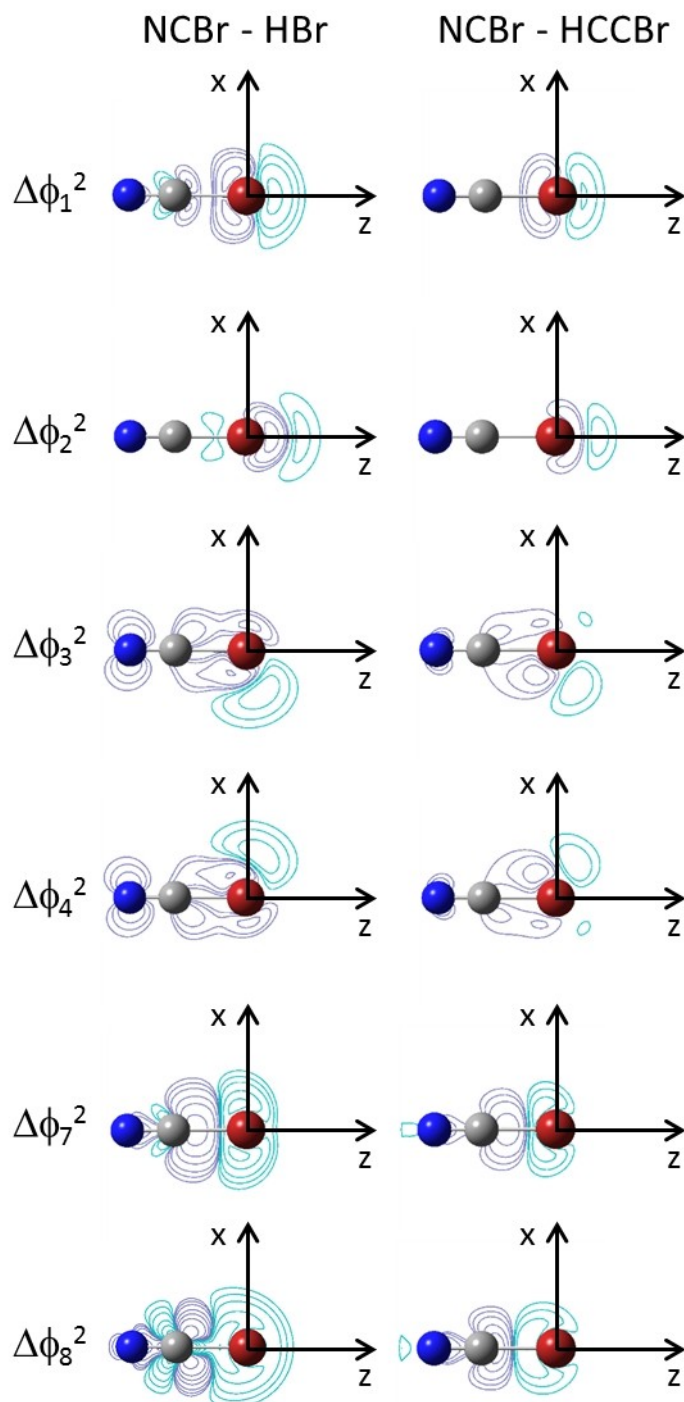


**Figure 3.** Plots of the differences between squared symmetry-unique SC orbitals of NCBBr and HBr (left), and NCBBr and HCCBr (right), with contour levels drawn at  $\pm 2, \pm 4, \pm 8 \times 10^9$  au, with  $n$  as an integer ranging from  $-4$  to  $0$ . Positive values are denoted by violet contours and negative values are denoted by cyan contours.

appearance of the  $\sigma$ -hole with respect to the Politzer's one.<sup>[5]</sup> By using molecular orbitals localized through the Edminston-Ruedenberg procedure, the authors report on the formation of three symmetry-equivalent  $sp^3$ -like orbitals on the halogen atom, which are responsible for the formation of the  $\sigma$ -hole in

the direction of the bond axis. This conclusion is in full agreement with the loss of the  $p_x$  and  $p_y$  symmetry shown by the SC orbitals.

In conclusion, by means of SC calculations we have here confirmed the qualitative model proposed by Politzer and

coworkers to explain the physical origin of halogen bonding,<sup>[4,5]</sup> putting it on a solid quantum mechanical basis and refining it by means of an accurate description of all the involved orbitals. The qualitative  $s^2p_x^2p_y^2p_z^1$  description of the electronic structure of the free bromine atom and its evolution after bonding with electron withdrawing groups is here fully generalized and quantitatively analyzed using the basic concepts of the VB approach. According to this study, the presence of the  $\sigma$ -hole on the halogen atom is associated with a contraction of the SC orbitals describing the  $p_z$  lone pair, while the negative belt around the halogen atom, observed only when bonded to electron-withdrawing groups of medium strength, is to be ascribed to a reduced contraction of the SC orbitals corresponding to the  $p_x$  and  $p_y$  lone pairs.

## Acknowledgements

A. G. acknowledges the French Research Agency (ANR) for financial support of the Young Researcher Project QuMacroRef through Grant No. ANR-17-CE29-0005-01.

## Conflict of Interest

The authors declare no conflict of interest.

**Keywords:** halogen bonding · valence bond theory · spin-coupled method · intermolecular interactions · quantum mechanics

- [1] a) D. B. Amabilino, D. K. Smith, J. W. Steed, *Chem. Soc. Rev.* **2017**, *46*, 2404–2420; b) T. F. A. de Greef, E. W. Meijer, *Nature* **2008**, *453*, 171–173; c) D. Philip, J. F. Stoddart, *Angew. Chem. Int. Ed.* **1996**, *35*, 1154–1196; *Angew. Chem.* **1996**, *108*, 1242–1286; d) J.-M. Lehn, *Science* **1985**, *227*, 849–856.
- [2] G. Cavallo, P. Metrangolo, R. Milani, T. Pilati, A. Priimagi, G. Resnati, G. Terraneo, *Chem. Rev.* **2016**, *116*, 2478–2601.
- [3] G. R. Desiraju, P. S. Ho, L. Kloo, A. C. Legon, R. Marquardt, P. Metrangolo, P. Politzer, G. Resnati, K. Rissanen, *Pure Appl. Chem.* **2013**, *85*, 1711–1713.
- [4] T. Clark, M. Hennemann, J. S. Murray, P. Politzer, *J. Mol. Model.* **2007**, *13*, 291–296.
- [5] P. Politzer, P. Lane, M. C. Concha, Y. Ma, J. S. Murray, *J. Mol. Model.* **2007**, *13*, 305–311.
- [6] For recent applications see, for example: a) C. Wang, D. Danovich, Y. Mo, S. Shaik, *J. Chem. Theory Comput.* **2014**, *10*, 3726–3737; b) T. Stuyver, D. Danovich, S. Shaik, *J. Phys. Chem. A* **2019**, *123*, 1851–1860; c) H. Zhang, C. Zhou, Y. Mo, W. Wu, *J. Comput. Chem.* **2019**, *40*, 1123–1129; d) F. E. Penotti, D. L. Cooper, P. B. Karadakov, *Int. J. Quantum Chem.* **2019**, *119*, e25845; e) S. Radenković, M. Antić, S. Đorđević, B. Braida, *Comput. Theor. Chem.* **2017**, *1116*, 163–173; f) S. Shaik, D. Danovich, P. C. Hiberty, *Comput. Theor. Chem.* **2017**, *1116*, 242–249.
- [7] a) J. Gerratt, W. N. Lipscomb, *Proc. Natl. Acad. Sci. USA* **1968**, *59*, 332–335; b) P. B. Karadakov, J. Gerratt, D. L. Cooper, M. Raimondi, *J. Chem. Phys.* **1992**, *97*, 7637–7655; c) D. L. Cooper, J. Gerratt, M. Raimondi, M. Sironi, T. Thorsteinsson, *Theor. Chim. Acta* **1993**, *85*, 261–270.
- [8] a) D. Jayatilaka, *Phys. Rev. Lett.* **1998**, *80*, 798–801; b) D. Jayatilaka, D. J. Grimwood, *Acta Crystallogr. Sect. A* **2001**, *57*, 76–86.
- [9] a) A. Genoni, D. Franchini, S. Pieraccini, M. Sironi, *Chem. Eur. J.* **2018**, *24*, 15507–15511; b) A. Genoni, G. Macetti, D. Franchini, S. Pieraccini, M. Sironi, *Acta Crystallogr. Sect. A* **2019**, *75*, 778–797.
- [10] D. Franchini, A. Genoni, F. Dapiaggi, S. Pieraccini, M. Sironi, *Int. J. Quantum Chem.* **2019**, *119*, e25946.
- [11] M. R. Scholfield, M. Coates Ford, C. M. Vander Zanden, M. Marie Billman, P. Shing Ho, A. K. Rappé, *J. Phys. Chem. B* **2015**, *119*, 9140–9149.
- [12] L. J. McAllister, D. W. Bruce, P. B. Karadakov, *J. Phys. Chem. A* **2012**, *116*, 10621–10628.

Manuscript received: March 5, 2020